

## THE FAR-INFRARED CONTINUUM OF QUASARS.

B.J. Wilkes<sup>1</sup>, E.J. Hooper<sup>1</sup>, K.K. McLeod<sup>2</sup>, M.S. Elvis<sup>1</sup>, C.D. Impey<sup>3</sup>, C.J. Lonsdale<sup>4</sup>,  
M.A. Malkan<sup>5</sup>, J.C. McDowell<sup>1</sup>

<sup>1</sup>Smithsonian Astrophysical Observatory, 60 Garden St., Cambridge, MA 02138, USA

<sup>2</sup>Astronomy Department, Wellesley College, Wellesley, MA 02481, USA.

<sup>3</sup>Steward Observatory, University of Arizona, Tucson, AZ 85721, USA

<sup>4</sup>IPAC, Caltech, Pasadena, CA 91125, USA

<sup>5</sup>Department of Astronomy, University of California, Los Angeles, CA 90095, USA

### ABSTRACT

ISO provides a key new far-infrared window through which to observe the multi-wavelength spectral energy distributions (SEDs) of quasars and active galactic nuclei (AGN). It allows us, for the first time, to observe a substantial fraction of the quasar population in the far-IR, and to obtain simultaneous, multi-wavelength observations from 5–200  $\mu\text{m}$ . With these data we can study the behavior of the IR continuum in comparison with expectations from competing thermal and non-thermal models. A key to determining which mechanism dominates, is the measurement of the peak wavelength of the emission and the shape of the far-IR–mm turnover. Turnovers which are steeper than  $\nu^{2.5}$  indicate thermal dust emission in the far-IR.

Preliminary results from our ISO data show broad, fairly smooth, IR continuum emission with far-IR turnovers generally too steep to be explained by non-thermal synchrotron emission. Assuming thermal emission throughout leads to a wide inferred temperature range  $\sim 50 - 1000\text{K}$ . The hotter material, often called the AGN component, probably originates in dust close to and heated by the central source, *e.g.* the ubiquitous molecular torus. The cooler emission is too strong to be due purely to cool, host galaxy dust, and so indicates either the presence of a starburst in addition to the AGN or AGN-heated dust covering a wider range of temperatures than present in the standard, optically thick torus models.

Key words: ISO; infrared astronomy; quasars.

### 1. INTRODUCTION AND ANALYSIS

The energy output of quasars and AGN is comparable throughout the far-IR to X-ray spectral regions, so studies of their emission mechanisms require observations throughout this range. Prior to ISO, the far-IR continuum was observed by IRAS, providing our first

look at quasars in this wavelength range and showing them to be strong emitters from 12–100  $\mu\text{m}$ . The poor spatial resolution and limited wavelength range of IRAS restricted observations to the IR-brightest subsets of quasars and AGN and left open many questions as to the range of behavior present and the emission mechanisms responsible in the various types of AGN. With ISO we are now able to address some of these limitations by studying a large number of different kinds of AGN and quasars.

We observed 72 quasars and AGN covering a full range of redshift and luminosity and many different types of SEDs. The observations were made with ISOPHOT (Lemke *et al.* (1996)) and cover 5–200  $\mu\text{m}$  in 8 bands. The status of this project, including a description of the sample and global comparisons of our results with those of IRAS, is summarised elsewhere (Hooper *et al.*, this volume). Here we discuss our preliminary results in the context of the scientific questions we wish to address, with particular emphasis on the high-redshift objects in the sample.

The data were processed with PIA (Gabriel *et al.* (1997))<sup>1</sup> through the AAP level, from which custom scripts (originating with M. Haas & S. Mueller at MPIA) were used to determine source fluxes and uncertainties. Default vignetting values from PIA were applied to the chopped data, and the flux scale was set by FCS observations. Sky noise estimates based on Herbstmeier *et al.* (1998) were included in the error budget. For further details of the data reduction please refer to Hooper *et al.* (this volume).

### 2. SPECTRAL ENERGY DISTRIBUTIONS (SEDs).

Figure 1 shows typical examples of the SEDs of a radio-loud (upper, RLQ) and radio-quiet (lower, RQQ) quasar (Elvis *et al.* (1994)). Throughout the far-IR–ultraviolet (UV) spectral region, the SEDs are remarkably similar, showing the big blue bump in the

<sup>1</sup>PIA is a joint development by the ESA Astrophysics Division and the ISOPHOT Consortium

optical-UV, the broad IR bump, and an inflection between the two centered at  $\sim 1 \mu\text{m}$ . The differences between the two centered at  $\sim 1 \mu\text{m}$ . The differences between the two radio classes are evident in the radio region where, by definition, the RLQs are several orders of magnitude more luminous, and in the soft X-ray region where the RLQs are a factor of  $\sim 3$  brighter and have a harder spectrum. This latter difference is generally ascribed to an additional synchrotron self-Compton component linked to the radio emission (see Wilkes (1999) for a review of quasar SEDs).

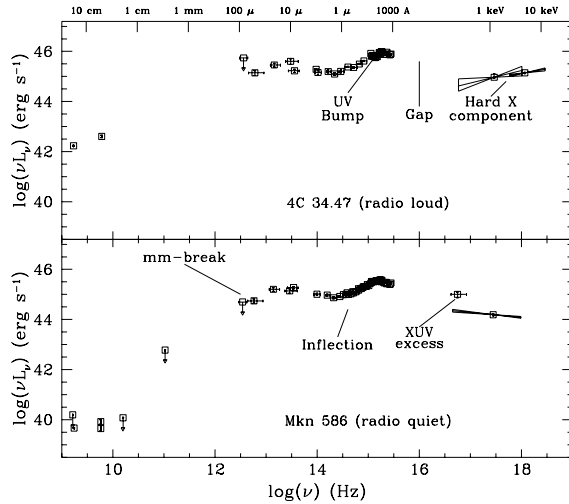


Figure 1. Rest-frame radio-X-ray spectral energy distributions (SEDs) for low-redshift radio-loud (upper, RLQ) and radio-quiet (lower, RQQ) quasars (Fig.1 from Elvis et al. (1994)). These are typical examples of SEDs in the current literature. The display of  $\nu L_\nu$  vs  $\nu$  highlights the energy output and the structure of the SED.

The radio-IR SEDs of core-dominated RLQs are generally smooth while in both RQQs and lobe-dominated RLQs the far-IR cutoff is steep and does not extrapolate into the radio. This difference has resulted in the general belief that the IR emission in core-dominated RLQs is dominated by beamed, non-thermal and in RQQs by thermal emission mechanisms (see Wilkes (1999) for a review). The median RLQ SED in Figures 2,3,4 was generated from a combination of lobe- and core-dominated RLQs. In a unification scenario (see Barthel (1999) for a review) the beamed IR component is expected to be weaker in lobe-dominated sources where the beam is in the plane of the sky. Thus it may not be surprising that the RLQ SED, formed by combining SEDs from the two radio subclasses, is similar to that of the RQQs. A detailed comparison of the SEDs of core- and lobe-dominated RLQs is required to confirm this scenario. Such a transition from non-thermal to thermal emission with decreasing core-dominance is demonstrated in the preliminary ISOPHOT results of the European Core Program on Quasars (Haas et al. (1998); see also this volume).

The main questions we wish to address with our ISO sample are (i) to better understand the interplay between thermal and non-thermal emission in the various types of source (ii) to investigate the relative contributions of cool (galactic/starburst) and warm

(AGN-related) dust (iii) to characterize and measure the continua in order to constrain models (iv) to study the evolution of the IR SEDs.

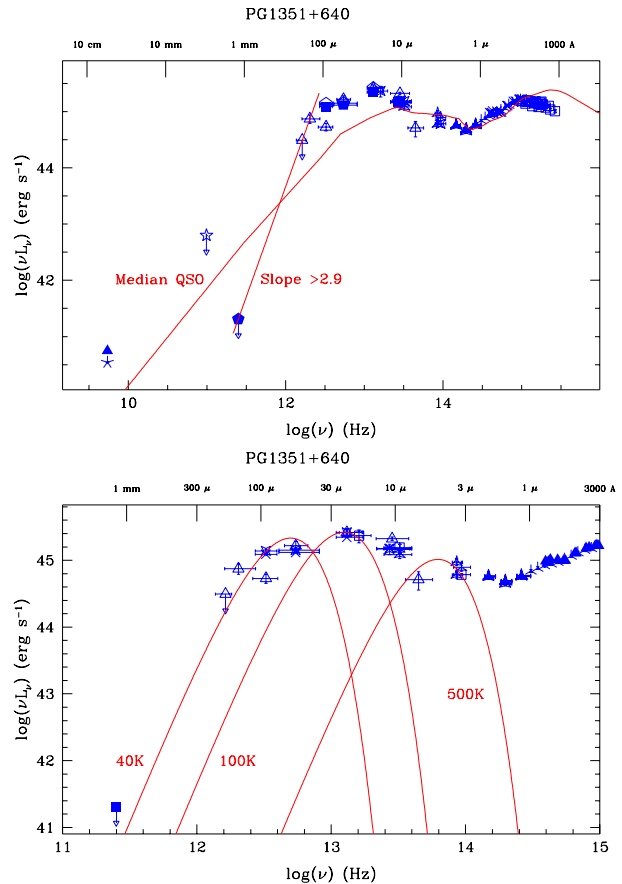


Figure 2. The rest-frame SED of the low-redshift ( $z=0.088$ ), RQQ PG1351+640 from Elvis et al. (1994) with the ISO data points (open triangles) added. **Upper:** the radio-UV SED showing a steep ( $\alpha_{fir} > 2.9$ ) far-IR cut-off; **Lower:** the IR-optical SED with representative grey body (assuming  $\beta = 2$ ) curves superposed.

## 2.1. LOW REDSHIFT QUASAR: PG1351+640

Figure 2 shows the rest-frame SED of a low-redshift ( $z=0.088$ ), RQQ PG1351+640. The ISO data points are shown as open triangles and the remainder of the multi-wavelength data are from Elvis et al. (1994). This SED is typical of the low-redshift RQQs in our sample and compares well with the low-redshift median. The current limit on the far-IR turnover is  $\alpha_{fir} > 2.9$ , too steep to be due to non-thermal synchrotron emission, for which  $\alpha_{fir} < 2.5$  is required and  $\alpha < 1$  is more typical (Gear et al. (1994)). We thus conclude that the far-IR emission in this quasars is dominated by thermal emission from dust.

The IR SED is smooth and indicates a wide and probably continuous range of temperatures: 40–500K. In a purely thermal scenario this smooth continuum can be explained by a combination of cool host galaxy dust, warm ( $\sim 100\text{K}$ ) starburst-related dust (e.g. Rowan-Robinson (1995)) and hot ( $T_{eff} \sim 800 - 1300\text{K}$ ) AGN-related dust (e.g. from a torus, Pier

Table 1. The Broad-band IR luminosities of the High redshift Quasars.

Name	Redshift	$L(7-25\ \mu\text{m})^1$	$L(2-25\ \mu\text{m})^1$	$L(2-200\ \mu\text{m})^1$	# ISO det's	ns
1107+48	3.010	1.7E+47	6.9E+47	-	2	
BR 1202-0727 <sup>2</sup>	4.690	1.7E+48	8.5E+48	8.9E+48	3	
1407+265	0.944	7.5E+46	1.2E+47	-	2	
1413+1143	2.551	8.8E+47	1.6E+48	2.0E+48	7	
1718+481	1.084	2.7E+46	8.2E+46	-	3	
HS 1946+7658	3.030	4.2E+47	1.1E+48	2.1E+48	4	
3C422	0.942	7.6E+46	1.4E+47	-	2	
1351+640	0.088	2.5E+45	3.1E+45	5.2E+45	6	

1: Luminosity over indicated bandpass, assuming  $H_o=50\ \text{km s}^{-1}\ \text{Mpc}^{-1}$  and  $q_o=0$  ( $\text{erg s}^{-1}$ )

2: Probably a gravitationally lensed source (Omont et al. (1996))

& Krolik (1993)). Alternatively the emission could originate in AGN-related dust which is sufficiently optically thick and/or geometrically arranged (e.g. the warped disk model of Sanders et al. (1989) or a patchy torus) to produce comparable emission over the wide range of observed temperatures. This latter scenario is supported by the results of van Bemmell & Barthel (this volume) which demonstrate that RLQs have significantly brighter far-IR emission than radio galaxies in samples which were matched so that the only difference should be one of orientation.

We also note that, with these data alone, we cannot rule out a significant contribution from a non-thermal component in the mid- and near-IR.

### 3. HIGH REDSHIFT QUASARS

Our sample includes 9 quasars with redshift  $> 0.9$ . The 7 for which we have reliable ISO detections are listed in Table 1 along with their redshifts, preliminary estimates of several broad-band IR luminosities and the number of ISO detections used in this determination. The luminosities were determined via linear interpolation between the data points and are not tabulated where there were insufficient data to provide useful constraints. The IR-band luminosities, determined assuming  $H_o=50\ \text{km s}^{-1}\ \text{Mpc}^{-1}$  and  $q_o=0$ , are high, ranging from  $10^{46-49}\ \text{erg s}^{-1}$  ( $\sim 10^{13-16}L_\odot$ ). For comparison, the low-redshift RQQ, PG1351+640 (Table 1) has luminosities  $\sim 10^{45}\ \text{erg s}^{-1}$  ( $\sim 10^{12}L_\odot$ ).

The rest-frame, radio-UV SED of BR 1202-0727, the object with the highest luminosity,  $L(2-200\ \mu\text{m}) \sim 10^{49}\ \text{erg s}^{-1}$ , is displayed in Figure 3. Our ISO fluxes and upper limits are shown as open triangles and our ground-based near-IR photometry, obtained at the Steward Observatory 61" telescope in March 1996, as open squares. Multiwavelength data are from Isaak et al. (1994) and McMahon et al. (1994). The median, low-redshift, RQQ SED (Elvis et al. (1994)), normalised at  $\sim 2\ \mu\text{m}$ , is superposed for comparison. Relative to the rest-frame optical emission, the IR emission in this object is  $\sim 2$  orders of magnitude stronger than is typical. This is a complex source. It is a luminous (dust  $\sim 10^{11}M_\odot$ , Ohta et al. (1996)), double (Omont et al. (1996)), CO source with a Ly $\alpha$  emission line companion (Hu et al. (1996)). Given its unprecedentedly strong mm and IR luminosities and double nature it seems highly likely that the source is gravitationally lensed and so amplified by  $\sim \times 10$ . However lensing can-

not explain the unusual SED of BR 1202-0727, since partial lensing would boost the smaller, optical/UV source rather than the probably extended IR emitting region.

Two extreme temperature grey-body curves (assuming an emissivity index,  $\beta = 2$ ) are also superposed in Figure 3 (upper) for illustration. Again a wide range of temperature is present, 50 – 1000K although the upper limits in the mid-IR prevent any constraint on the emission at intermediate temperatures in this source. In Figure 3 (lower) an SED representing a ULIRG with the maximum H-band host galaxy luminosity based on low redshift quasars (McLeod (1997)) is superposed. This comparison illustrates that the far-IR emission is comparable or in excess of that expected from a ULIRG and far exceeds that expected from the host galaxy (see also Wilkes (1997)).

The rest-frame, radio-UV SED of HS 1946+7658 is displayed in Figure 4. Our ISO fluxes and upper limits are shown as open triangles and the remainder of the multiwavelength data were taken from Kuhn et al. (1994) and Kuhn (1996). We also superpose grey-body curves (assuming dust with emissivity index,  $\beta = 2$ ) at two extreme temperatures to illustrate the range of temperature present in the data. The SED of HS 1946+7658 is remarkably similar to the low redshift, RQQ median, extending the conclusion of Kuhn et al. (1994) based on the optical SED for this source. As with the low redshift RQQ PG1351+640, the IR continuum appears smooth. In a pure thermal scenario, this suggests the presence of dust covering a continuous range from  $\sim < 80 - 500\text{K}$  rather than two distinct low and high temperature components. The low temperature limit is determined by the longest wavelength at which we have data rather than a real cut-off in the source.

In summary, the broad-band IR luminosities, ranging from  $10^{46-48}\ \text{erg s}^{-1}$  ( $\sim 10^{13-15}L_\odot$ , assuming BR 1202-0727 is lensed), are  $\sim 2$  orders of magnitude higher than those of Ultraluminous IR galaxies (ULIRGs) whose SEDs peak in the IR with luminosities  $\sim 10^{11-13}L_\odot$  (e.g. Sanders & Mirabel (1996)), even allowing for the different assumed Hubble constant (Sanders & Mirabel (1996) use  $H_o = 75\ \text{km s}^{-1}\ \text{Mpc}^{-1}$ ). In the far-IR these luminosities are too high to be due to the host galaxy. As for the low redshift sources (2.1.), the inferred temperature ranges are generally too broad to be fit by standard, AGN molecular torus models (Pier & Krolik (1993)), which can reproduce the higher temperature emission. Thus more complex models or a strong starburst component are required to provide the lower temperature emission.

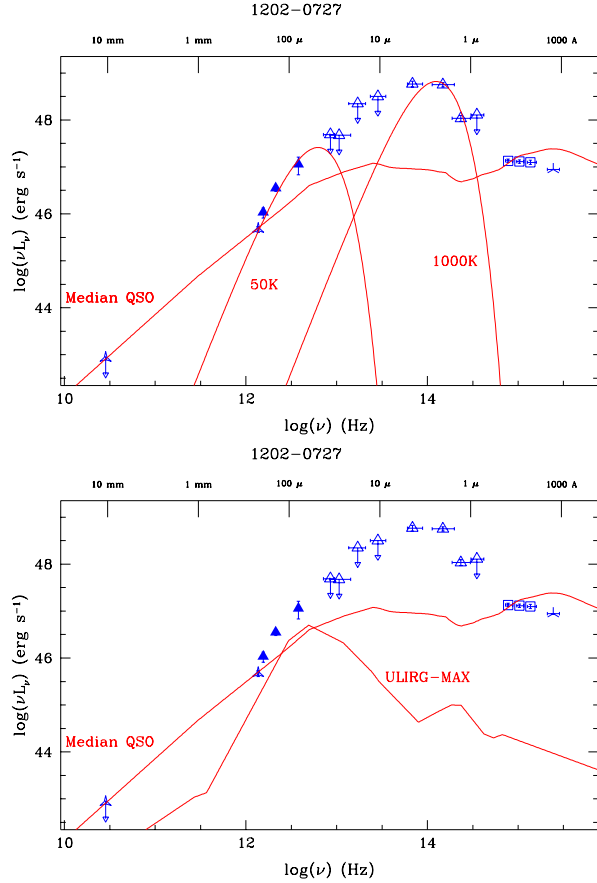


Figure 3. The rest-frame, radio-UV SED of the high-redshift, RQQ BR 1202-0727 including the ISO data points (open triangles). The median SED for low redshift RQQs (Elvis et al. (1994)), normalised to the optical SED, is superposed for comparison. **Upper:** grey-body curves (assuming  $\beta=2$ ) at two extreme temperatures are superposed **Lower:** the SED of an ULIRG is superposed, normalised to the highest H-band luminosity host galaxy observed in low redshift sources (McLeod (1997)).

#### ACKNOWLEDGMENTS

We wish to thank the staff at the ISOPHOT data center in Heidelberg, in particular Martin Haas, for their help and hospitality while working on these data. We also thank the ISO staff at IPAC for their continual support and help both during visits and remotely. This work is supported by NASA grant NAGW-3134.

#### REFERENCES

Barthel, P. 1999 in “Quasars and Cosmology”, Gary Ferland and Jack Baldwin, Eds, ASP Conf. Proc. *in press*

Elvis, M. S., Wilkes, B. J., McDowell, J. C., Green, R. F., Bechtold, J., Willner, S. P., Cutri, R., Oey, M. S., & Polonski, E. 1994, ApJS, 95, 1

Gabriel, C. et al. 1997 in Proceedings of ADASS VI, ASP Conf. Ser. 125, G. Hunt & H.E. Payne, eds., [ASP], p. 108

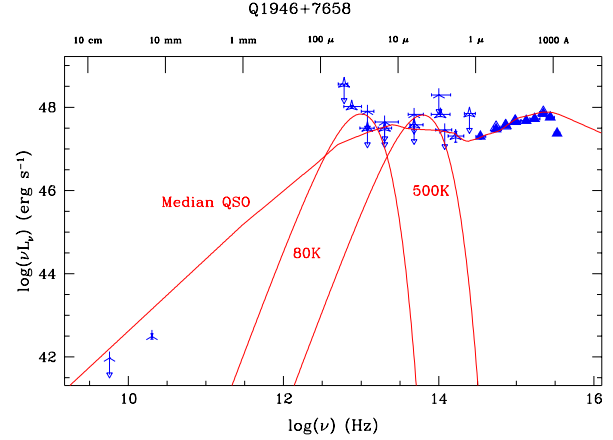


Figure 4. The rest-frame, radio-UV SED of the high-redshift, RQQ HS 1946+7658 including the ISO data points shown as open triangles. The median SED for low redshift RQQs (Elvis et al. (1994)) is superposed for comparison. Grey-body curves (assuming  $\beta=2$ ) at two temperatures are superposed to illustrate the range of temperature present in a pure thermal emission scenario.

Gear, W., Stevens, J.A., Hughes, D.H., Litchfield, S.J., Robson, E.I., Terasanta, H., Valtaoja, E., Steppe, H., Aller, M.F., & Aller, H.D. 1994, MNRAS, 267, 167

Herbstmeier, U., Abraham, P., Lemke, D., Laureijs, R. J., Klaas, U., Mattila, K., Leinert, C., Surace, C. & Kunkel, M. 1998, AA, 332, 739

Haas, M., Chini, R., Meisenheimer, K., Stickel, M., Lemke, D., Klaas, U. & Kreysa, E. 1998 ApJL, 503, 109

Hu, E.M., McMahon, R.G. & Egami, E. 1996, ApJ, 459, L53

Isaak, K.G., McMahon, R.G., Hills, R.E. & Withington, S. 1994, MNRAS, 269, L28

Kuhn, O. 1996, PhD Thesis, Harvard University

Kuhn, O., Bechtold, J., Cutri, R., Elvis, M. & Reike, M. 1994, ApJ, 438, 643

Lemke, D. et al. 1996, AA 315, L64

McLeod, K.K. 1997 in “Quasar Hosts”, D.L. Clements & I. Perez-Fournon eds., [Springer], p. 45

McMahon, R.G., Omont, A., Bergeron, J., Kreysa, E. & Haslam, C.G.T. 1994, MNRAS, 267, L9

Ohta, K., Yamada, T., Nakanishi, K., Kohno, K., Akiyama, M. & Kawabe, R. 1996, Nature, 382, 426

Omont, A., Petitjean, P., Guilloteau, S., McMahon, R.G., Solomon, P.M. & Pecontal, E. 1996, Nature, 382, 428

Pier, E.A. & Krolik, J.H. 1993, ApJ, 418, 673

Rowan-Robinson, M. 1995, MNRAS, 272, 737

Sanders, D.B. & Mirabel, I.F. 1996, ANRAA, 34, 749

Sanders, D., Phinney, E.S., Neugebauer, G., Soifer, B.T., & Matthews, K. 1989, ApJ, 347, 29

Wilkes, B.J. 1999 in “Quasars and Cosmology”, Gary Ferland and Jack Baldwin, Eds, ASP Conf. Proc. *in press*

Wilkes, B.J. 1997 in “Quasar Hosts”, D.L. Clements & I. Perez-Fournon eds., [Springer], p. 136